# Performance Analysis of Photonically Generated Microwave Signal using a Dual-parallel Dual-drive Mach-Zehnder Modulator in Dispersive Media

Amitesh Kumar, Vishnu Priye and Kowshik Moyya
*Department of Electronics Engineering, Indian School of Mines Dhanbad, 826004, India*

Keywords: Microwave Photonics, Modulator, Optoelectronics and Dispersion.

Abstract: Dispersion is one of the potential limiting parameter for generation of microwave signal using photonic methods. In this paper, we analyse theoretically, the influence of fiber dispersion parameter on the photonically generated microwave/millimeter wave signal using dual-parallel dual-drive $LiNbO_3$ Mach-Zender modulators. Intensity at the output of photodetector having, eight and sixteen times frequency of microwave drive signal and harmonic suppression versus modulation index (β) and filter attenuation is discussed and it has been found that dispersion plays a major role on generation and transmission of microwave signal in optical domain.

## 1 INTRODUCTION

Microwave Photonics (MWP) systems are emerging as a new aspect for generation and transmission of microwave and millimeter wave signal in optical domain for applications such as broad-band wireless communication system, modern instrumentation, bio-medical, radar, warfare systems, and recently for THz Technology. There are various advantages of photonic generation of the microwave signal like high band-width, large tunability and immune to electromagnetic interference over conventional technique in electrical domain (Yao, 2009; Seeds and Williams, 2006). The low frequency modulated double-sideband (DSB) optical signal suffers less from the chromatic dispersion of the fiber than that of the high frequency modulated signal when transmitted through standard single mode fiber (SSMF) (Schmuck, 1995; Gliese et al., 1996; Smith et al., 1997) and high frequency signal generated by DSB technique is limited by the bandwidth of the optical sources like laser diode or the external modulator and the fiber chromatic dispersion (Hofstetter et al., 1995). To overcome these limitations, a photonic generation method that uses narrow bandwidth optical components to generate high frequency electrical signals is one of the promising solutions now a day. Electrical signal generation based on optical heterodyning can be achieved by using either two stable lasers or one laser with external optical modulator. The electrical signal generation by beating two free running lasers may meet system application specifications but is of poor quality (spectral response). Optical injection locking and optical phase-locked loop (OPLL) (Yao, 2010) have been proposed to improve the signal quality. Methods using a laser with external optical modulator, such as optical intensity modulator or optical phase modulator (O'reilly et al,. 1992; Qi et al., 2005) have shown great potential for producing high purity, high-frequency microwave/millimeter-wave signals. Frequency octupled millimeter-wave signal is proposed using dual-parallel Mach-Zehnder (DPMZD) and a wavelength fixed optical notch filter (Zhang and Pan, 2012). Recently a microwave signal generation using dual-parallel dual-drive Mach-Zehnder modulator having frequency, sixteen times of microwave drive signal is proposed (Kumar and Priye, 2014).

One of the most limiting factor in microwave photonics systems are dispersion that deteriorate the performance of generated microwave signal. The dispersion analysis of reported work (Kumar and Priye, 2014) is proposed and demonstrated for beat frequency of $4^{th}$ and $8^{th}$ order optical sidebands, obtained at the output of respective photo detectors.



Kumar, A., Priye, V. and Moyya, K.
Performance Analysis of Photonically Generated Microwave Signal using a Dual-parallel Dual-drive Mach-Zehnder Modulator in Dispersive Media.
DOI: 10.5220/0005741702640269
In *Proceedings of the 4th International Conference on Photonics, Optics and Laser Technology (PHOTOPTICS 2016)*, pages 266-271
ISBN: 978-989-758-174-8

## 2 PROPOSED MODEL AND ANALYSIS

In this proposed approach, shown in Figure 1, light wave emitted from a tunable laser source (TLS) is launched into to a DPMZM which is driven by two amplified RF signal with phase difference of $\boldsymbol{\pi/2}$. The bias voltage of the two arms of upper and lower dual-drive $\mathbf{LiNbO_3}$ MZM are at 0 V and phase difference between the RF signal of two arms of each modulator is $\boldsymbol{\pi}$ i.e., MZM is biased at maximum transmission point (MATP) to suppress all the odd-order optical sidebands. The output of DPMZD is passed through fibre Bragg grating (FBG) wavelength fixed notch filter which is tuned to attenuate optical carrier of frequency $\boldsymbol{\omega_0}$ with attenuation factor α in dB and splitted into two paths. From the Figure 1, the splitted signal is launched into the upper and lower photo detectors ($PD_1$ & $PD_2$) through optical amplifier (EDFA) and optical fiber of length 25 km. If the intensity of optical carrier and modulation index is small only the 4th and 8th order sidebands will be significant at the input of $PD_1$ and at the input of $PD_2$, 8th and 16th order sideband will be significant after rejection of 4th order sidebands through optical band reject filter, considering high optical carrier intensity and significant modulation index. A beat signal with eight and sixteen times the frequency of the electrical drive signal is generated at photo detectors, $PD_1$ and $PD_2$ respectively. The power of suppressed sidebands at the output of DPMZM is transferred into the even-order sidebands (4th, 8th and 16th), improving the signal generation efficiency.

The output electric field from the dual-drive $LiNbO_3$ Mach-Zehnder modulator is given as (Dai et al. 2013)

$$E_{out}(t) = \frac{1}{2}E_0 \exp(j\omega_0 t)\left[\exp\left(j\pi\left(\frac{V_1(t)}{V_{\pi RF}} + \frac{V_{Bias1}}{V_{\pi DC}}\right)\right) + \exp\left(j\pi\left(\frac{V_2(t)}{V_{\pi RF}} + \frac{V_{Bias2}}{V_{\pi DC}}\right)\right)\right] \quad (1)$$

Where $E_0$ and $\boldsymbol{\omega_0}$ are, the electric field & angular frequency of the input optical carrier respectively, $\boldsymbol{V_{\pi RF}}$ is switching voltage, $\mathbf{V_{\pi DC}}$ is switching bias voltage, $\mathbf{V_{Bias1}}$ and $\mathbf{V_{Bias2}}$ are the DC bias voltage between two arms, and $\mathbf{V_1(t)}$ & $\mathbf{V_2(t)}$ are the RF modulating electrical signal voltage. $\mathbf{V_1(t)}$ and $\mathbf{V_2(t)}$ can be expressed as two sinusoidal functions; $\mathbf{V_1(t) = A_1 cos(\omega_{RF} t)}$ and $\mathbf{V_2(t) = A_2 cos(\omega_{RF} t + \varphi)}$, where $\boldsymbol{A_1}$ and $\boldsymbol{A_2}$ are the amplitude of the two RF signals, $\boldsymbol{\omega_{RF}}$ is the frequency of modulating RF signal, and $\boldsymbol{\varphi}$ is the phase difference between two RF signals.

The optical field at the output of the DPMZM can be expressed as

$$\begin{aligned} E_{out\,DPMDM}(t) = {} & \sqrt{2}\,E_0 J_0(\beta)\cos(\omega_0 t) + \\ & \sum_{n=1}^{\infty}\sqrt{2}\,E_0 J_{4n}(\beta)[\cos(\omega_0 t - 4n\omega_{RF} t) + \cos(\omega_0 t + 4n\omega_{RF} t)] + \\ & \sum_{n=1}^{\infty}\sqrt{2}\,E_0 J_{8n}(\beta)[\cos(\omega_0 t - 8n\omega_{RF} t) + \cos(\omega_0 t + 8n\omega_{RF} t)] + \\ & \sum_{n=1}^{\infty}\sqrt{2}\,E_0 J_{16n}(\beta)[\cos(\omega_0 t - 16n\omega_{RF} t) + \cos(\omega_0 t + 16n\omega_{RF} t)] \end{aligned} \quad (2)$$

Where $J_{4n}$, $J_{8n}$ and $J_{16n}$ are the Bessel function of the first kind and of order $4n, 8n$ and $16n$ respectively, and $\beta$ is the phase modulation index (PMI). For $0 < \beta < 2$, the Bessel functions $J_{8n}(\beta)$ and $J_{16n}(\beta)$ for $n \geq 2$ are much smaller than $J_8(\beta)$ and $J_{16}(\beta)$. Therefore, it is reasonable to ignore the optical sidebands with order higher than 16 in our analysis, so only the carrier, $\pm 4^{th}$, $\pm 8^{th}$ and $\pm 16^{th}$ order sidebands are left.

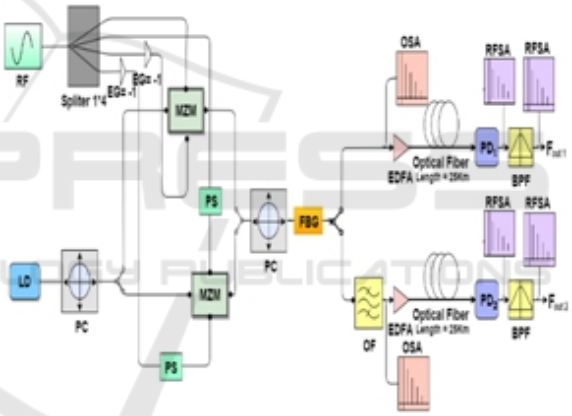


Figure 1: Schematic of the proposed microwave signal generation system. (LD: laser diode; RF: radio frequency; PC: polarization controller; MZM: Mach-Zehnder Modulator; EG: electrical gain; PS: phase shift $90^0$; OF: Optical band reject filter; PD: photo detector; BPF: band pass filter).

The Figure 2, illustrates the optical spectra at the output of DPMZM, since the two sidebands originated from the same optical and microwave sources, an excellent phase correlation is maintained. Beating the two sidebands at a PD, a high-spectral-purity signal, eight times as well as sixteen times frequency of microwave drive electrical signals is obtained.

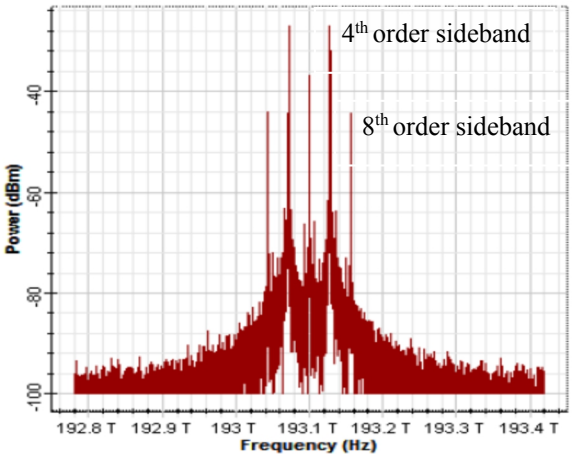


Figure 2: The spectrum of the modulated optical signal at the output of DPMZM using OptiSystem software (Kumar and Priye 2014).

## 2.1 Performance Analysis in Dispersive Media

It is known that in a wide-band electrical heterodyning system purity of generated signal is main concern. The generated electrical signal at the PD, $V_{out}$ can be expressed as

$$V_{out1}(t) = RJ_4^2(\beta)\cos(8\omega_{RF}) \quad (3)$$

$$V_{out2}(t) = RJ_8^2(\beta)\cos(16\omega_{RF}) \quad (4)$$

Where R is a constant that is related to the responsivity of the photodetector (PD). Since the two optical sidebands originate from the same optical source, the frequency stability and phase noise of the generated signal are mainly determined by the electrical drive signal. Equation (3) and (4) also shows that the amplitude of the generated electrical signal can be maximized by optimizing the value $J_4^2$ and $J_8^2$ respectively.

Assuming that, all unwanted odd-order and even order optical sidebands generated by the modulation of the DPMZM due to microwave drive radio frequency signal, completely suppressed by using a suitable dc-bias voltage and the attenuation of the optical notch filter at its notch wavelength is α dB. From equation (2), the optical signal at the output of the FBG optical notch filter can be written as

$$\begin{aligned} E_{out\,DPMDM}(t) = {} & \sqrt{2}\,E_0 k J_0(\beta)\cos(\omega_0 t) + \\ & \textstyle\sum_{n=1}^{\infty}\sqrt{2}\,E_0 J_{4n}(\beta)[\cos(\omega_0 t - 4n\omega_{RF} t) + \\ & \cos(\omega_0 t + 4n\omega_{RF} t)] + \\ & \textstyle\sum_{n=1}^{\infty}\sqrt{2}\,E_0 J_{8n}(\beta)[\cos(\omega_0 t - 8n\omega_{RF} t) + \\ & \cos(\omega_0 t + 8n\omega_{RF} t)] + \\ & \textstyle\sum_{n=1}^{\infty}\sqrt{2}\,E_0 J_{16n}(\beta)[\cos(\omega_0 t - 16n\omega_{RF} t) + \\ & \cos(\omega_0 t + 16n\omega_{RF} t)] \end{aligned} \quad (5)$$

Where k is the optical field attenuation factor, which is related as $\alpha = -20\log_{10} k$.

Generally, for a commercially available MZM, the maximum available phase modulation index $\beta_{max}$ is 2. When $0 \le \beta \le 2$, Bessel function $J_{4n}$, $J_{8n}$ & $J_{16n}$ for $n \ge 1$ are all monotonically increasing with respect to β and monotonically decreasing with respect to the order of Bessel function n, and $J_4(2) = 0.033996$, $J_8(2) = 0.00002218$ and $J_{16}(2) = 4.5060e-014$. Hence, it is reasonable to ignore the optical sideband with a Bessel coefficient higher than $J_{16}(\beta)$ for significant amplitude of optical carrier and microwave drive (RF) signal in our discussion. Therefore, equation (5) can be further simplified as

$$\begin{aligned} E_{out\,DPMDM}(t) = {} & \sqrt{2}\,E_0 k J_0(\beta)\cos(\omega_0 t) + \\ & \sqrt{2}\,E_0 J_4(\beta)[\cos(\omega_0 t - 4\omega_{RF} t) + \cos(\omega_0 t + 4\omega_{RF} t)] + \\ & \sqrt{2}\,E_0 J_8(\beta)[\cos(\omega_0 t - 8\omega_{RF} t) + \cos(\omega_0 t + 8\omega_{RF} t)] + \\ & \sqrt{2}\,E_0 J_{16}(\beta)[\cos(\omega_0 t - 16\omega_{RF} t) + \cos(\omega_0 t + 16\omega_{RF} t)] \end{aligned} \quad (6)$$

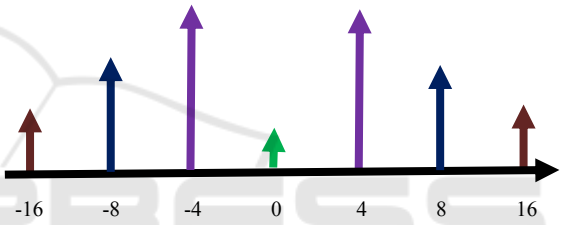


Figure 3: Illustration of the electrical spectrum at the output of a PD.

Equation (6) shows that the optical signal consists of an attenuated optical carrier and six optical sidebands. The spectrum of this optical signal is illustrated as shown in Figure 3. The arrow direction shows that initial phase with respect to the phase of optical carrier before transmission.

When the optical signal shown in Figure 3 is transmitted over a single-mode fiber, the chromatic dispersion of the fiber will cause an extra phase shift to each optical sideband compare to the optical carrier. By expanding the propagation constant $\beta(\omega)$ of the fiber for each optical sideband to a Taylor series around the angular frequency of the optical carrier (Okamoto 2000), i.e.

$$\beta(\omega_0 \pm 4n\omega_{RF}) = \beta(\omega_0) + \beta^1(\omega_0)(\pm 4n\omega_{RF}) + \frac{1}{2}\beta^2(\omega_0)(\pm 4n\omega_{RF})^2 + \cdots \quad (7)$$

$$\beta(\omega_0 \pm 8n\omega_{RF}) = \beta(\omega_0) + \beta^1(\omega_0)(\pm 8n\omega_{RF}) + \frac{1}{2}\beta^2(\omega_0)(\pm 8n\omega_{RF})^2 + \cdots \quad (8)$$

$$\beta(\omega_0 \pm 16n\omega_{RF}) = \beta(\omega_0) + \beta^1(\omega_0)(\pm 16n\omega_{RF}) + \frac{1}{2}\beta^2(\omega_0)(\pm 16n\omega_{RF})^2 + \cdots \quad (9)$$

Where $\beta^1(\omega_0)$ and $\beta^2(\omega_0)$ are the first and second-order derivative of the propagation constant $\beta(\omega_0)$ at angular frequency $\omega_0$, respectively. The effect of higher order dispersion is neglected for the single-mode fiber at 1552nm band (Marshall, Crosignani and Yariv 2000) and $\beta^2(\omega_0)$ can be expressed by the chromatic dispersion parameter D as

$$\beta^2(\omega_0) = -\frac{c}{2\pi f_0^2} D \quad (10)$$

Where c is the speed of light in vacuum and $f_0$ is the frequency of the optical carrier.

The electric field at the end of the transmission over single-mode fiber of length L can be obtained by adding the transmission phase delay $\beta(\omega_0 \pm 4n\omega_{RF})L$ , $\beta(\omega_0 \pm 8n\omega_{RF})L$ and $\beta(\omega_0 \pm 16n\omega_{RF})L$ to the corresponding optical sideband shown in (6). Electrical harmonic will be generated by applying this optical signal to a photodiode. The power intensities (Qi et al. 2005) of the 8th and 16th order electrical harmonic $I_8$ and $I_{16}$ respectively are proportional to the coefficient of optical sidebands.

$$I_8 \propto \frac{E_0^4}{2}\left\{J_4^2(\beta) + 2kJ_0(\beta)J_8(\beta)\cos\left[64\pi cDL\left(\frac{f_{RF}}{f_0}\right)^2\right]\right\}^2 \quad (11)$$

$$I_{16} \propto \frac{E_0^4}{2}\left\{J_8^2(\beta) + 2kJ_0(\beta)J_{16}(\beta)\cos\left[256\pi cDL\left(\frac{f_{RF}}{f_0}\right)^2\right]\right\}^2 \quad (12)$$

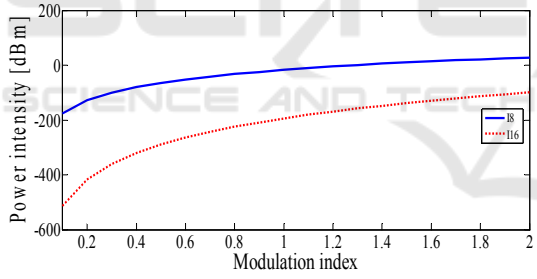


(a)

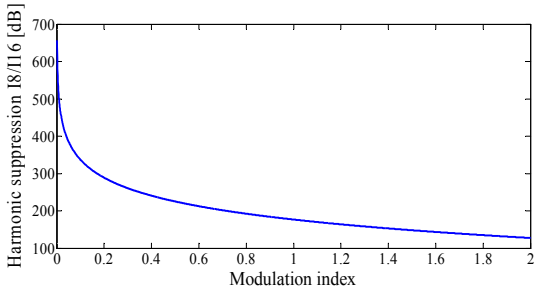


(b)

Figure 4: Power intensity and harmonic suppression versus modulation index (a) Power intensity $I_8$ & $I_{16}$, eighth and sixteenth order harmonics. (b) Harmonics suppressions $I_8/I_{16}$. (Frequency of the electrical drive.$f_{RF} = 7$ GHz.).

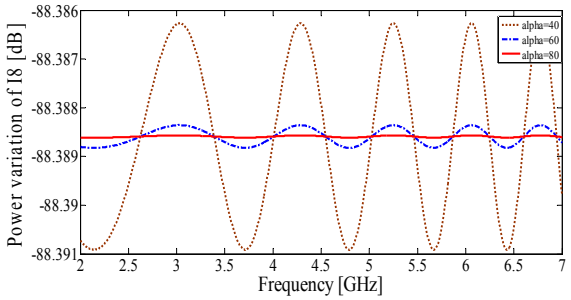


(a)

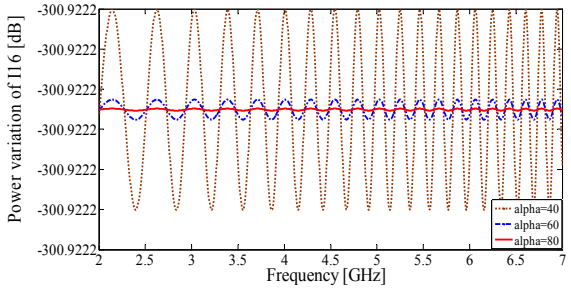


(b)

Figure 5: Power variation versus frequency of the electrical drive signal. (a) Power variation of $I_8$, (b) Power variation of $I_{16}$. (Modulation index $\beta = 0.6$).

For a distribution system that operate at 1552.52 nm with a transmission distance of 25 km over a standared single mode fiber with $D = 17\ ps/(nm.km)$, the power intensity $I_8$ ,$I_{16}$ and harmonics suppression of $I_8/I_{16}$ verses the modulation index $\beta(0 \leq \beta \leq 2)$ are plotted in Figure 4.

From figure 4(a) the power intensity of 8th and 16th order harmonics are monotonically increases for $0 \leq \beta \leq 2$ and Figure 4(b) show that the harmonic suppression $I_8/I_{16}$ is monotonically decreases for $0 \leq \beta \leq 2$, which is independent of the attenuation $\alpha$ of optical notch filter.

Figure 5(a) and 5(b) shows the power variation of the generated electrical signals $I_8$ and $I_{16}$ respectively, which is due to the combined effect of the limited attenuation of the optical carrier and the chromatic dispersion of the fiber when tuning the frequency of the electrical drive signal from 2 to 7 GHz. It is clearly seen that when $\alpha \geq 40dB$, this power variation is smaller. This means the amplitude of the eight and sixteen times of microwave drive signals are stable over the tuning band when $\beta$ is a constant and $\alpha$ is greater than equal to 40 dB.

## 2.2 Analysis for Higher Order Dispersion

By expanding the propagation constant $\beta(\omega)$ of the

fiber for each optical sideband to a Taylor series around the angular frequency of the optical carrier up to 5th order dispersion (Okamoto 2000), i.e.,

$$\beta(\omega_0 \pm 2n\omega_{RF}) = \beta(\omega_0) + \beta^1(\omega_0)(\pm 2n\omega_{RF})^1 + \frac{1}{2}\beta^2(\omega_0)(\pm 2n\omega_{RF})^2 + \frac{1}{6}\beta^3(\omega_0)(\pm 2n\omega_{RF})^3 + \frac{1}{24}\beta^4(\omega_0)(\pm 2n\omega_{RF})^4 + \frac{1}{120}\beta^5(\omega_0)(\pm 2n\omega_{RF})^5 \quad (13)$$

The third order dispersion parameter is given by

$$\beta^3(\omega_0) = \frac{d^2\tau}{d\omega^2} = \frac{\lambda^2}{(2\pi c)^2}\left[\lambda^2\frac{\partial^2\tau}{\partial\lambda^2} + 2\lambda\frac{\partial\tau}{\partial\lambda}\right] = \frac{\lambda^2}{(2\pi c)^2}[\lambda^2 D_1 + 2\lambda D] \quad (14)$$

Where D is Group Velocity Dispersion (GVD) and $D_1$ is the Dispersion Slope.
The fourth order dispersion parameter is given by (Keiser 2008)

$$\beta^4(\omega_0) = \frac{d^3\tau}{d\omega^3} = \frac{\lambda^3}{(2\pi c)^3}[\lambda^3\frac{\partial^3\tau}{\partial\lambda^3} + 6\lambda^2\frac{\partial^2\tau}{\partial\lambda^2} + 6\lambda\frac{\partial\tau}{\partial\lambda}] = \frac{\lambda^3}{(2\pi c)^3}[\lambda^3 D_2 + 6\lambda^2 D_1 + 6\lambda D] \quad (15)$$

The fifth order dispersion parameter is given by (Keiser 2008)

$$\beta^5(\omega_0) = \frac{d^4\tau}{d\omega^4} = \frac{\lambda^4}{(2\pi c)^4}[\lambda^4\frac{\partial^4\tau}{\partial\lambda^4} + 12\lambda^3\frac{\partial^3\tau}{\partial\lambda^3} + 36\lambda^2\frac{\partial^2\tau}{\partial\lambda^2} + 24\lambda\frac{\partial\tau}{\partial\lambda}] = \frac{\lambda^4}{(2\pi c)^4}[\lambda^4 D_3 + 12\lambda^3 D_2 + 36\lambda^2 D_1 + 24\lambda D] \quad (16)$$

The electric field at the end of the transmission over single-mode fiber of length L can be obtained by adding the transmission phase delay $\beta(\omega_0 \pm 4n\omega_{RF})L$ , $\beta(\omega_0 \pm 8n\omega_{RF})L$ and $\beta(\omega_0 \pm 16n\omega_{RF})L$ to the corresponding optical sideband shown in (6). Electrical harmonic will be generated by applying this optical signal to a photodiode. The power intensities (Qi et al., 2005) of the 8th and 16th order electrical harmonic $I_8$ and $I_{16}$ respectively for higher order dispersion are proportional to the coefficient of optical sidebands

$$I_8 \propto \frac{E_0^4}{2}\left\{J_4^2(\beta) + 2kJ_0(\beta)J_8(\beta)\cos\left[\frac{1}{2}\beta^2(\omega_0)(8\omega_{RF})^2 + \frac{1}{24}\beta^4(\omega_0)(8\omega_{RF})^4\right]\right\}^2 \quad (17)$$

$$I_{16} \propto \frac{E_0^4}{2}\left\{J_8^2(\beta) + 2kJ_0(\beta)J_{16}(\beta)\cos\left[\frac{1}{2}\beta^2(\omega_0)(16\omega_{RF})^2 + \frac{1}{24}\beta^4(\omega_0)(16\omega_{RF})^4\right]\right\}^2 \quad (18)$$

## 3 RESULTS AND DISCUSSION

In our calculation, we used the electrical drive signal frequency nearly equal to 7 GHz, optical carrier of 193.1 THz, modulation index ($\beta$) range of 0-2 for the MZM and assumed the initial phase of the electrical drive signal for the MZM equal to zero. Referring to ITU's G.655 fiber (ITU-T 2009); Fiber chromatic dispersion, D = 0.5ps/km-nm, Dispersion curvature, $D_1$ = 0.085ps/km-nm², Dispersion curvature, $D_2$ = 2.3776x10$^{-4}$ ps/km-nm$^3$, Electrical field attenuation factor, $\alpha$ =100 dB, Gain of EDFA= 100 and Electric field strength, $E_0$ = 10V/m.

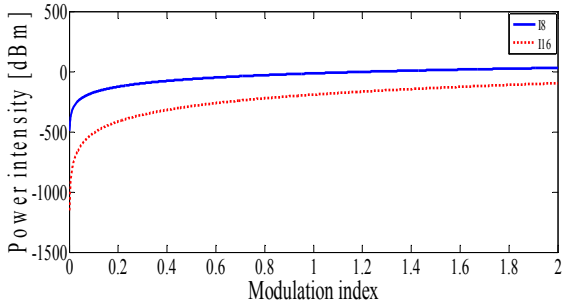


Figure 6: Power intensity $I_8$ & $I_{16}$, eighth and sixteenth order harmonics.

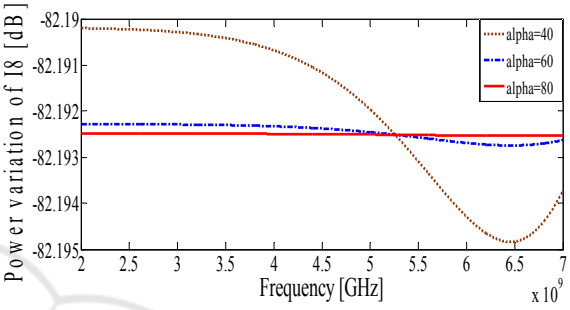


Figure 7: Power variation ($I_8$) versus frequency of the electrical drive signal.

## 4 CONCLUSIONS

In this paper, the detail theoretical analysis of influence of fiber dispersion on photonically generated microwave/millimeter wave using dual-parallel dual-drive $LiNbO_3$ Mach-Zender modulators is investigated. Performance analysis of eighth and sixteen orders harmonics generated from microwave drive signal (RF) on SSMF and ITU's G.655 fiber of length 25 km are calculated theoretically and it is observed that dispersion parameters have significant impact on microwave/millimeter wave signal generation using photonic technique. The impact decreases as the order of dispersion term increases.

## REFERENCES

Yao, J., 2009. Microwave photonics. Lightwave Technology, Journal of,27(3), pp.314-335.

Seeds, A.J. and Williams, K.J., 2006. Microwave photonics. Lightwave Technology, Journal of, 24(12), pp.4628-4641.

Schmuck, H., 1995. Comparison of optical millimetre-wave system concepts with regard to chromatic dispersion. Electronics Letters, 31(21), pp.1848-1849.

Gliese, U., Norskov, S. and Nielsen, T.N., 1996. Chromatic dispersion in fiber-optic microwave and millimeter-wave links. Microwave Theory and Techniques, IEEE Transactions on, 44(10), pp.1716-1724.

Smith, G.H., Novak, D. and Ahmed, Z., 1997. Overcoming chromatic-dispersion effects in fiber-wireless systems incorporating external modulators. Microwave Theory and Techniques, IEEE Transactions on,45(8), pp.1410-1415.

Hofstetter, R., Schmuck, H. and Heidemann, R., 1995. Dispersion effects in optical millimeter-wave systems using self-heterodyne method for transport and generation. Microwave Theory and Techniques, IEEE Transactions on,43(9), pp.2263-2269.

Yao, J., 2010. Microwave photonics: Photonic generation of microwave and millimeter-wave signals. International Journal Of Microwave And Optical Technology, 5(1), pp.16-21.

O'reilly, J.J., Lane, P.M., Heidemann, R. and Hofstetter, R., 1992. Optical generation of very narrow linewidth millimetre wave signals. Electronics Letters, 28(25), pp.2309-2311.

Qi, G., Yao, J., Seregelyi, J., Paquet, S. and Bélisle, C., 2005. Generation and distribution of a wide-band continuously tunable millimeter-wave signal with an optical external modulation technique. Microwave Theory and Techniques, IEEE Transactions on, 53(10), pp.3090-3097.

Zhang, Y. and Pan, S., 2012, September. Experimental demonstration of frequency-octupled millimeter-wave signal generation based on a dual-parallel Mach-Zehnder modulator. In Microwave Workshop Series on Millimeter Wave Wireless Technology and Applications (IMWS), 2012 IEEE MTT-S International (pp. 1-4). IEEE.

Kumar, A. and Priye, V., 2014, December. Photonic Generation of Microwave Signal Using a Dual-Parallel Dual-Drive Mach-Zehnder Modulator. In International Conference on Fibre Optics and Photonics (pp. S5A-66). Optical Society of America.

Dai, B., Gao, Z., Wang, X., Chen, H., Kataoka, N. and Wada, N., 2013. Generation of versatile waveforms from CW light using a dual-drive Mach-Zehnder modulator and employing chromatic dispersion. Lightwave Technology, Journal of, 31(1), pp.145-151.

Okamoto, K., 2000. Fundamentals of optical waveguides. Academic press, pp 72-72.

Marshall, W.K., Crosignani, B. and Yariv, A., 2000. Laser phase noise to intensity noise conversion by lowest-order group-velocity dispersion in optical fiber: exact theory. Optics letters, 25(3), pp.165-167.

Keiser, G., 2008. Optical fiber communications. Mcgraw-Hill, Singapore.

ITU-T, R., 2009. G. 655. Characteristics of Non Zero dispersion shifted single mode optical fiber cable, p.13.